A New Method for the Registration of Cardiac PET and MR Images Using Deformable Model Based Segmentation of the Main Thorax Structures

Timo Mäkelä[1,2], Patrick Clarysse[2], Jyrki Lötjönen[3], Outi Sipilä[4], Kirsi Lauerma[4], Helena Hänninen[5,7], Esa-Pekka Pyökkimies[1], Jukka Nenonen[1], Juhani Knuuti[6], Toivo Katila[1,7], and Isabelle E. Magnin[2]

[1] Laboratory of Biomedical Engineering, Helsinki University of Technology, P.O.B. 2200, FIN-02015 HUT, Finland
{Timo.Makela, Toivo.Katila}@hut.fi
[2] CREATIS, INSA, Batiment Blaise Pascal, 69621 Villeurbanne Cedex, France
{Patrick.Clarysse, Isabelle.Magnin}@creatis.insa-lyon.fr
[3] VTT Information Technology, P.O.Box 1206, FIN-33101 Tampere, Finland
Jyrki.Lotjonen@vtt.fi
[4] Department of Radiology, Helsinki University Central Hospital, P.O.B. 340, FIN-00029 HUS, Finland
[5] Division of Cardiology, Helsinki University Central Hospital, P.O.B. 340, FIN-00029 HUS, Finland
[6] Turku PET Centre, c/o Turku University Central Hospital, Box 52, FIN-20521, Finland
[7] BioMag Laboratory, Helsinki University Central Hospital, P.O.B. 503, FIN-00029 HUS, Finland

Abstract. Integration of magnetic resonance (MR) and positron emission tomography (PET) images of the heart has proved its usefulness for the estimation of the myocardial viability. In this paper, a method for the rigid registration of cardiac MR and PET images is presented. It is based on the matching of the surfaces of thorax structures extracted by a deformable model from PET transmission and MR transaxial images. MR short axis registration with PET emission image is easily derived and allows the study viability in the proper anatomic conditions. The method has been evaluated on ten patients suffering from three vessel coronary artery disease. Qualitative results were good with 9 over the 10 available cases. A quantitative estimation of the registration quality confirmed the nice abilities of this approach.

1 Introduction

The combination of multiple cardiac image modalities like Magnetic Resonance Imaging (MRI) and Positron Emission Tomography (PET), has gained an increasing interest for physiologic understanding and diagnostic purposes, specially

W. Niessen and M. Viergever (Eds.): MICCAI 2001, LNCS 2208, pp. 557–564, 2001.

for viability studies. The combination requires the geometric alignment i.e. registration of multimodal images. This is a difficult problem mainly due to the continuous motion of the heart. Methods to correlate PET cardiac studies by using a surface based image registration technique of PET transmission images has been presented in [1] and [2]. In this work, we propose a new method for cardiac transaxial and short axis (SA) MR and PET image registration. A preliminary approach has been presented in [3]. Here, the method has been greatly improved by substituting the manual segmentation of the thorax structures by a deformable model based automatic segmentation. The data and the method are presented in section 2. The registration results are presented in section 3 and discussed in section 4.

2 Material and Method

2.1 Data

The data set is composed of MR and PET images of ten patients suffering from three vessel coronary artery disease [4]. Mean age was 69 (8 men, 2 women). All patients underwent MR and fluorine-18-deoxyglucose (FDG) PET imaging within 10 days. The MR imaging was performed at the Department of Radiology of Helsinki University Central Hospital with a 1.5 T Siemens Magnetom Vision imager (Siemens, Erlangen, Germany). A series of 39 ECG-gated contiguous transaxial images was acquired during free respiration using TurboFLASH sequence with the body array coil (Fig. 1a). The pixel size and the slice thickness were 1.95 x 1.95 mm and 10 mm, respectively. Five ECG-gated breath-hold cine SA slices covering the ventricles were also acquired. The pixel size for SA slices was 1.25 x 1.25 mm and the slice thickness 7 mm with a gap of 15 mm between slices (Fig. 1b).

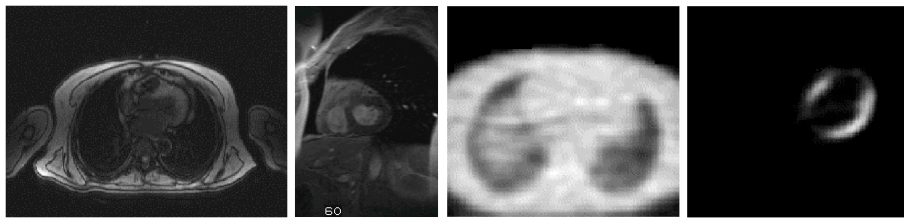

Fig. 1. (a) Transaxial and (b) SA MR images of the thorax and heart, (c) PET transmission and (d) emission images.

PET imaging was performed at the Turku PET Centre using a Siemens ECAT 931/08-12 (Siemens/CTI, Knoxville, USA) PET scanner. A series of 16 contiguous transmission and emission images was acquired. The pixel size and the slice thickness were 2.41 x 2.41 mm and 6.75 mm, respectively (Fig. 1c, d).

2.2 Registration Protocol

The proposed registration method is based on the matching of the thorax and lungs surfaces which are visible in both PET transmission and MR transaxial images. The registration protocol first matches PET transmission and transaxial MR images and then computes the SA PET slices that correspond to the SA MR slices. The main steps are:
1) Image resizing to get the same isotropic voxel dimensions. Tri-linear interpolation was used.
2) Segmentation of the thorax and lungs was performed for the transaxial MR and PET transmission images by a deformable model based method [5] which is summarized in subsection 2.3.
3) Selection of a set of points from the segmented surfaces of the thorax and lungs in the PET model. The uniformly distributed nodes of the deformable model were used.
4) Calculation of the rigid registration parameters (3 translations, 3 rotations) to find the best matching between the point set and the surface of the segmented MR image. The minimization algorithm is explained in subsection 2.4.
5) Registration of the PET emission image to the transaxial MR image using the computed registration parameters.
6) Registration of SA MR images with PET data. Slice position information contained in the MR image header provides the transformation between transaxial MR and SA MR slices. The SA PET slices corresponding to SA MR images are computed using the estimated parameters of the transformation.

2.3 Deformable Model Based Segmentation

The segmentation of the thorax structures is based on the elastic deformation of a topologic and geometric prior model using a multiresolution approach [5]. A thorax model including full triangulated thorax and lungs surfaces was used with transaxial MR images (Fig. 2a). With the transmission PET images, a truncated model with only a part of the thorax was used (Fig. 2b).

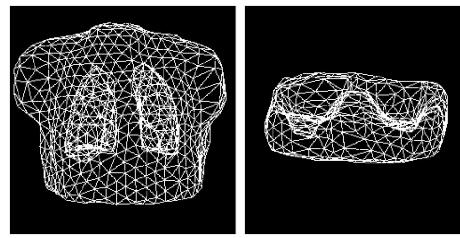

(a) (b)

Fig. 2. Geometric and topologic prior model of the thorax for (a) transaxial MR and (b) transmission PET image segmentation.

The deformation algorithm adapts the prior model to locally fit the salient edges in the image within a minimization process. The energy to be minimized is

$$E_{total} = E_{image} + \gamma E_{model}, \tag{1}$$

where E_{image} represents the matching error between the prior model and the partial edges in the data volume. E_{model} tends to preserve the model's shape by restricting the deformation of the prior model. It describes the deviation of the model's surface normals from their original orientation. The image energy results from a distance map [6] built upon edges extracted either by a Canny-Deriche method [7] or image thresholding. In order to select corresponding edges with the model, oriented distance maps [5] were used. The parameter γ sets the contribution of the two energy components. A multiresolution process speeds up the minimization of the energy and improves the convergence.

2.4 Estimation of the Rigid Transformation

The 6 rigid registration parameters (3 translations, 3 rotations) result from the best match between the set of the nodes of the triangulated surfaces extracted from the PET transmission image and the surfaces of the segmented MR image. The optimal transformation minimizes the sum of the distances between the transformed points and a distance map built upon the segmented MR surfaces using the chamfer distance transformation [6].

For the sake of simplicity, the minimization algorithm is described here only for 2 parameters representing, for example, the translation in x- and y-directions on a 2-D plane. The extension to 6 parameters is straightforward. The parameters to be optimized form the parameter vector (t_1, t_2). The optimal parameter vector is iteratively searched in the discrete search space. The initial position for the parameter vector is (t_{1o}, t_{2o}) (Fig. 3). The iteration steps for the search of a new parameter vector are as follows:
1) Possible values for the parameter t_k, k∈[1,2] are t_k-gd_k, t_k-(g-1)d_k,.. t_k, .., t_k+gd_k, where g is a user-defined positive integer parameter affecting the number of the possible new values, and parameter d_k (positive real number) represents the magnitude by which the parameter t_k is varied.
2) For all $(2g+1)^n$ combinations of the parameter vector, where n is the number of parameters (big dots in Fig. 3), the cost function is computed.
3) A user-defined number of combinations, m, having the lowest registration error, are selected for the new initial parameter vectors (selected positions of step 1, Fig. 3).
4) Each d_k-component is divided by 2.
5) Steps 1-2 are repeated for all m initial parameter vectors. Then, steps 3-4 provides an new local optima. Therefore, the number of initial parameter vectors remains constant during the iterations. Iterations are repeated until the cost function does not decrease more than a user-predefined value ϵ.

The algorithm does not necessarily converge to a global minimum of the cost function. However, the method samples the search-space more than a basic gradient descent method and allows find a minimum with a higher probability. The sampling of the search space is controlled by the parameters g and d_k. In addition, the computation time is only a few seconds, which is generally not the case with global optimization algorithms.

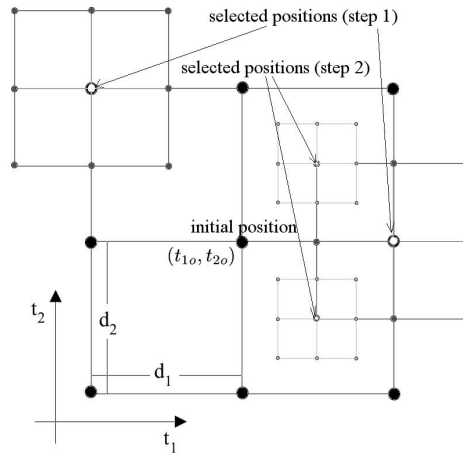

Fig. 3. Principle for the search of the optimal translation parameters.

3 Results

3.1 Segmentation Results

Three multiresolution levels were used (for image data, model and deformation grid). Canny-Deriche method or image thresholding were used for the edge extraction. Fig. 4 presents the segmentation results of case E1 for MR (top) and PET transmission image (down). Segmentation results (white contours) are compared to manual delineation (gray contours).

3.2 Registration Results

Fig. 5 presents the registration result obtained with the E1 case. SA PET images which correspond to the MR SA image planes are computed using the obtained registration parameters. In Figs. 6 and 7 registered end-diastolic MR and PET emission images are presented in the transaxial and SA planes, respectively.

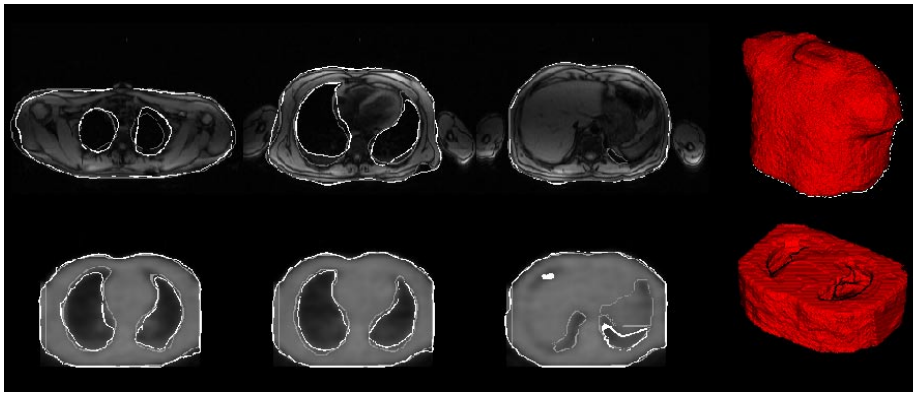

Fig. 4. Segmentation results of transaxial MR (top) and PET transmission (down) images for case E1. White contours correspond to the deformable model based segmentation and gray contours show the manual delineation. A 3-D visualization [8] of the corresponding deformable model based segmentation is shown on the right.

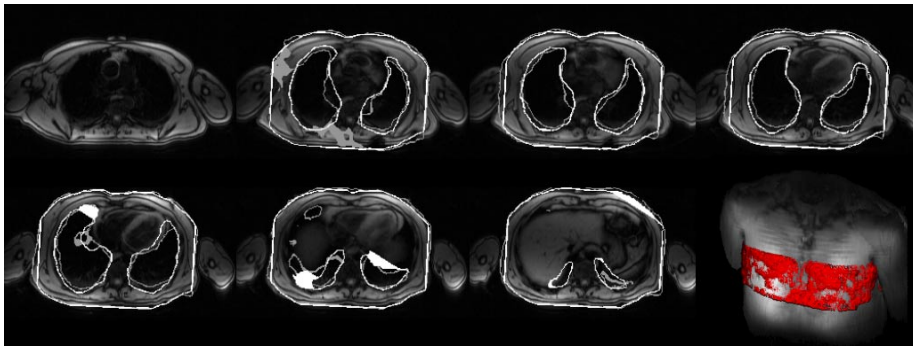

Fig. 5. Contours from registered PET images are superimposed onto the MR transaxial image plane. Automatically segmented contours are shown in white and manually delineated in gray. Bottom right corner: A 3D visualization illustrates the positioning of the registered PET transmission data relatively to the ray traced MR thorax image.

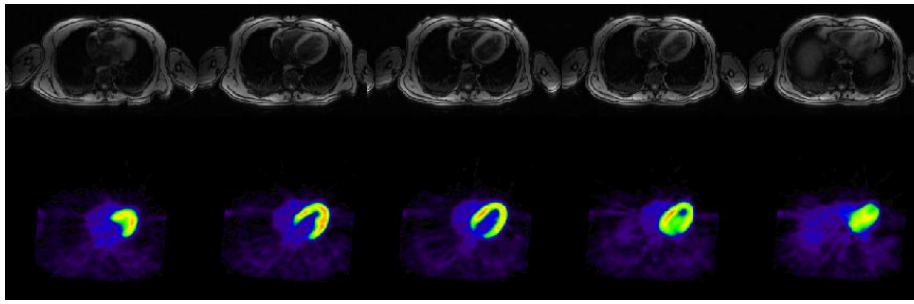

Fig. 6. Registered transaxial end-diastolic MR (top) and PET emission (bottom) image slices for the E1 case.

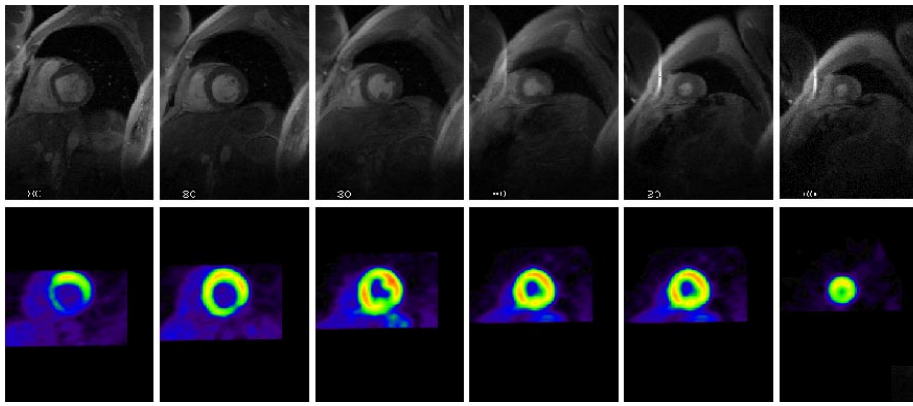

Fig. 7. Registered end-diastolic SA MR (top) and PET emission (bottom) image slices.

4 Discussion and Conclusion

The proposed method was applied to the 10 available cases. It did give visually good results for 9 cases out of the 10. In the failing case, there were unexpected artifacts in the FDG PET data. In order to quantitatively evaluate the algorithm, the statistics of the distance between registered PET surface points and segmented MR image surface were computed. When using deformable model based automatic segmentation, registration error was 2.8 ± 0.5 mm (minimum 1.9 and maximum 3.8 mm). With the manual delineation of the thorax structures, registration error was 2.4 ± 0.9 mm (minimum 0.5 and maximum 3.5 mm). Although this computed error term mainly quantify the difference between segmentation results of PET and MR thorax models, it gives a reasonable index of the quality of the registration in the absence of a reference data set.

Due to the presence of arms in MRI and their absence in PET, we did exclude points of the PET model located on the thorax sides for the calculation of the registration parameters. Initial parameter vector should also be close enough for the algorithm to converge to optimal result. This was the case in all of the studies since the positioning of the patient was identical in both imaging modalities, and as a result, the initial alignment of the MR distance map volume and the PET model was similar.

We did not observe major differences between registration based on manual delineation and automatic segmentation. In some cases, registration based on manual delineation performed better. One possible reason for this is that sometimes the automatic deformable model based segmentation locally fails to follow deep cavities. One additional segmentation step using a denser deformation grid could help to solve this problem.

The automatic segmentation of the MR and PET images with size 256 x 256 x 217 voxels takes less than 3 minutes on a PC workstation (PIII, 800 MHz). With the same image size, the execution time for registration was about 50

seconds when about 400 points were selected to compute the rigid transformation parameters. The speed of registration algorithm depends on factors like the need of the preprocessing, the complexity of the cost function and the number of the cost function evaluations performed by the optimization algorithm [10]. Compared to the iterative closest point (ICP) algorithm [9], our approach also requires the segmentation of the data. In our method, the distance map is computed once as a preprocessing step and after that the estimation of the distances between the model and the data points is immediate. On the contrary, in the ICP algorithm, distances are explicitly computed at every iteration. In our experiments the proposed registration parameter search strategy did provide a fast and reliable results. In future works, we will compare current method to other registration methods and also validate this method by using simulated images.

References

1. Pallotta S., Gilardi M. C., Bettinardi V., Landoni C., Striano G., Masi R. and Fazio F.: Application of a surface matching image registration technique to the correlation of cardiac studies in positron emission tomography (PET) by transmission images. Phys. Med. Biol., **40** (1995) 1695–1708.
2. Kim R., Aw T., Bacharach S., Bonow R.: Correlation of cardiac MRI and PET images using lung cavities as landmarks. Computers in Cardiology, (1991) 49–52.
3. Mäkelä T., Clarysse P., Lötjönen J., Sipilä O., Hänninen H., Nenonen J., Lauerma K., Knuuti J., Katila T. and Magnin I. E.: A method for registration of cardiac MR and PET images for the myocardial viability study. In: Marzullo, P. (ed.): NATO advanced research workshop - Understanding Cardiac Imaging Techniques From Basic Pathology to Image Fusion. NATO Science Series: Life and Behavioural Sciences. Vol. 332. IOS Press (2001) 155–165.
4. Lauerma K., Niemi P., Hänninen H., Janatuinen T., Voipio-Pulkki L., Knuuti J., Toivonen L., Mäkelä T., Mäkijärvi M. A. and Aronen H. J.: Multimodality MR imaging assessment of myocardial viability: combination of first-pass and late contrast enhancement to wall motion dynamics and comparison with FDG-PET. Radiology, **217** (2000) 729–736.
5. Lötjönen J., Reissman P.-J., Magnin I.E. and Katila T.: Model extraction from magnetic resonance volume data using the deformable pyramid. Medical Image Analysis, **4** (1999) 387–406.
6. Borgefors G.: Hierarchical chamfer matching: A parametric edge matching algorithm. IEEE Trans. Pattern Anal. Machine Intell., **6** (1988) 849–865.
7. Canny J.: A computational approach to edge detection. IEEE Trans. Pattern Anal. Machine Intell., **8** (1986) 679–698.
8. Pyökkimies E. P, Salli E. and Katila T. Fast image order volume rendering algorithm for multimodal image visualization. In: Nenonen J., Ilmoniemi R.J. and Katila T. (eds.): Biomag2000, Proc. 12th Int. Conf. on Biomagnetism, (2001) 1043–1045.
9. Besl P.J. and McKay N.D.: A method for regisration of 3-D shapes. IEEE Trans. Pattern Anal. Machine Intell., **14** (1992) 239–256.
10. Van Herk M.: Image registration using chamfer matching. In: Bankman I. N. (ed.): Handbook of medical imaging. Academic Press (2000) 515–527 .